Materials Today Chemistry 40 (2024) 102252

Contents lists available at ScienceDirect

Materials Today Chemistry

journal homepage: www.journals.elsevier.com/materials-today-chemistry/

Flame-retardant and tough poly(lactic acid) with well-preserved mechanical strength *via* reactive blending with bio-plasticizer and phosphorus derivative

Zimeng Zhang [a], Siqi Huo [b,*], Guofeng Ye [a], Cheng Wang [a], Qi Zhang [a], Zhitian Liu [a,**]

[a] Hubei Engineering Technology Research Center of Optoelectronic and New Energy Materials, School of Materials Science & Engineering, Wuhan Institute of Technology, Wuhan, 430205, China
[b] School of Engineering, Centre for Future Materials, University of Southern Queensland, Springfield, 4300, Australia

ARTICLE INFO

Keywords:
Polylactic acid
Reactive blending
Flame retardancy
Toughness
Thermal stability

ABSTRACT

With sustainable development, advanced poly(lactic acid) (PLA) with superior toughness and flame retardancy is highly demanded in various industries, but the current design strategies often fail to achieve such bioplastics. In this work, flame-retardant and tough PLA bioplastics with well-preserved thermal stability and mechanical strength and enhanced UV resistance and soil degradation are prepared by solvent-free, reactive blending of PLA, bio-based epoxidized soyabean oil (ESO) and 9,10-dihydro-9-oxa-10-phosphaphenanthrene 10-oxide (DOPO). With the introduction of 10.0 wt% ESO and 3.0 wt% DOPO, the resultant PLA/10E/3D bioplastic has a high tensile strength of 52.8 MPa, with 26.3 times and 67.5 % increases in elongation at break and impact strength compared to those of PLA due to the toughening effect of ESO and the rigid structure of DOPO. The superior toughness of PLA/10E/3D enables it to outperform previous flame-retardant PLA counterparts. PLA/10E/3D achieves a vertical burning (UL-94) V-0 classification and a limiting oxygen index (LOI) of 27.5 %, indicative of satisfactory flame retardancy. Compared with PLA, PLA/10E/3D maintains high thermal stability and shows significantly enhanced UV-protecting and soil degradation properties. Therefore, this work delivers a green and scalable reactive processing method to create flame-retardant, tough yet strong bioplastics with improved soil decomposition and UV resistance, which contributes to sustainable development.

1. Introduction

The ubiquitous applications of non-degradable petroleum plastics have brought about the depletion of oil resources and increasingly severe environmental problems. In response to sustainable development strategies, the development of biodegradable bioplastics have gained more and more attention in recent years, such as poly(butylene adipate-*co*-terephthalate) (PBAT) [1,2], polybutylene succinate (PBS) [3], and PLA [4,5]. Among them, PLA has realized practical applications because of its high mechanical strength, biocompatibility, and wide raw material sources. However, the poor toughness and intrinsic flammability of PLA have obviously limited their high-tech applications [6].

Considering green development, the common strategy to increase the toughness of PLA is to blend it with bio-based flexible polymers or plasticizers. For instance, Ding et al. [7] introduced 5 wt% of polycaprolactone (PCL) into PLA to fabricate a tough PLA composite. Their results showed that the notch impact strength of the resulting PLA composite can be up to 251 kJ/m^2. Recently, Liu et al. [8] reported toughened PLA (PLA/PBAT/DCP/PEG600DA) composites by blending PLA with dicumyl peroxide (DCP), poly(ethylene glycol) 600 diacrylate (PEG600DA) and PBAT. The impact strength and elongation at break of PLA/PBAT/DCP/PEG600DA reached 44.2 kJ/m^2 and 290 %, respectively. Although these PLA systems feature superior toughness and high biomass content, they usually suffer from low tensile strength and poor flame retardancy, which reduces their practical values. Introducing phosphorus derivatives into PLA has been considered a promising approach to address the flammability issue of PLA due to their low smoke and toxicity, environmental friendliness, and high flame-retardant efficiency [9–14]. For example, aluminum hypophosphite (ALHP), ammonium polyphosphate (APP), DOPO, etc., have

* Corresponding author.
** Corresponding author.
E-mail addresses: Siqi.Huo@unisq.edu.au, sqhuo@hotmail.com (S. Huo), able.ztliu@wit.edu.cn (Z. Liu).

https://doi.org/10.1016/j.mtchem.2024.102252
Received 10 June 2024; Received in revised form 31 July 2024; Accepted 13 August 2024
Available online 17 August 2024

been utilized in the fire-resistant PLA, but as-prepared PLA systems showed unsatisfied mechanical performances because the phosphorus-derived flame retardants will catalyze the decomposition of PLA in the melt-blending process. Therefore, efforts should be intensified to the creation of high-performance PLA combining superior toughness and flame retardancy.

Recently, some toughened and flame-retardant PLA systems have been reported, but most of them involve complex synthesis processes and require large amounts of organic solvents and expensive petroleum-based raw materials, which violates ecologically sustainable development [15–22]. Therefore, we chose the low-cost, bio-based epoxy soybean oil (ESO) as a toughening agent [23–28], and the commercial phosphorus-derived DOPO as a flame retardant to develop toughened and flame retardant PLA bioplastics by simple reactive blending in this work. Since PLA contains the terminal –COOH group, ESO contains the epoxy group, and DOPO possesses the P–H group, they can undergo *in-situ* grafting reaction during melt blending to ensure the homogeneous dispersion of ESO and DOPO in the PLA matrix. As-fabricated PLA/10E/3D with 10.0 wt% of ESO and 3.0 wt% of DOPO exhibits superior toughness, with impact strength and elongation at break of 6.7 kJ/m^2 and 106.3 %. Additionally, it achieves enhanced flame retardancy with a UL-94 V-0 rating, with an LOI of 27.5 %. Because of the covalent linkages between PLA, ESO, and DOPO, PLA/10E/3D displays comparable thermal stability to PLA. The introduction of DOPO and ESO brings about the enhanced UV-shielding and soil-decomposition performances of PLA/10E/3D. Hence, this work provides a feasible and eco-friendly strategy for creating high-performance, flame-retardant, tough PLA bioplastics with enhanced soil degradation and UV protection, and well-preserved thermal stability and mechanical strength, which can find wide applications in modern industries.

2. Experimental section

2.1. Materials

Poly(lactic acid) (3052D) was purchased from Nature-Works LLC (USA). Epoxidized soya bean oil (ESO, Epoxy value > 6.0) and 9,10-dihydro-9-oxa-10-phosphaphenanthrene 10-oxide (DOPO, 97 %) were supplied by Shanghai Energy Chemical Co., Ltd. (China). All chemicals were applied as received.

2.2. Fabrication of PLA composites

Firstly, the PLA granules were dried in a vacuum at 80 °C for 12 h to remove moisture. The dried PLA granules were added to the torque rheometer, followed by ESO, and then continuously mixed for 10 min at 200 °C and 70 rpm. DOPO was then introduced, and blended for 10 min. The resultant solid products were heat-compressed at 200 °C under a pressure of 14 MPa into different shapes according to the testing specimen size requirements. The sample is named PLA/xE/xD, where E, D and x represents ESO, DOPO, and their mass ratio, respectively. The fabrication procedures of PLA, PLA with 10.0 wt% ESO (PLA/10E), and PLA with 3 wt% DOPO (PLA/3D) were identical to that of PLA/xE/xD. The detailed formulations are tabulated in Table 1.

Table 1
The formulations of different PLA samples.

Sample	PLA (wt%)	ESO (wt%)	DOPO (wt%)
PLA	100.0	0	0
PLA/10E	90.0	10.0	0
PLA/3D	97.0	0	3.0
PLA/7.5E/3D	89.5	7.5	3.0
PLA/10E/3D	87.0	10.0	3.0
PLA/15E/3D	82.0	15.0	3.0

2.3. Characterization

The differential scanning calorimetry (DSC) was carried out by a DSC Q600 apparatus (TA Instruments, USA) at a ramp rate of 10 °C/min from 30 to 250 °C. Fourier transform infrared (FTIR) spectrometry was carried out using a Nicolet 6700 Fourier transform spectrometer (Thermo Fisher, USA) with potassium bromide pellets. Liquid nuclear magnetic resonance (NMR) spectroscopy was recorded on Bruker Advance III 500 MHz spectrometer (Bruker Corporation, Switzerland) at room temperature using $CDCl_3$ as solvent containing 0.03 % v/v tetramethylsilane (TMS). According to ASTM D638, the tensile stress-strain plots were investigated on an INSTRON 5966 universal test machine (USA) at a crosshead speed of 5 mm/min. To ensure data reliability, the reported data were the average of at least five specimens. For the notched Izod impact test, it was undertaken on a LIANXIANG impact testing machine (China) based on GB/T 1843–2008. The scanning electron microscopy (SEM) observation was undertaken at 15 kV on an EOL JSW-5510LV instrument (Japan), which was coupled with an energy dispersion X-ray (EDX) spectrometer. The specimens need to be gold-plated before SEM observation. The thermogravimetric analysis (TGA) was carried out on a NETZSCH STA449F3 facility (Germany). During this test, 5.0–10.0 mg of the powdered specimen was heated from 30 °C to 800 °C at a constant rate of 20 °C/min under N_2 condition. The optical performances of PLA films with the size of 50 mm × 50 mm × 0.2 mm were studied using a Lambda35 UV spectrometer (PerkinElmer, USA). The UV-protection factor (UPF) of the film was specifically calculated according to GB/T 18830-2009. The soil degradation behaviors of PLA and PLA/10E/3D were investigated by burying them in a 7.0 cm deep soil with a green plant and watering every three days (water volume: 500 mL). The gel permeation chromatography (GPC) and SEM observation were conducted on original specimens and samples after 30 and 75 days of burial. The GPC measurement was conducted *via* a Waters 1525 GPC facility (USA) with an elution agent of $CHCl_3$ and a flow rate of 1.0 mL/min. The limiting oxygen index was recorded on a Jiangning JF-3 equipment (China), and the sample was 100 mm × 6.5 mm × 3.0 mm in size. The vertical combustion test was performed on a Jiangning CFZ-3 facility (China), and the specimen size was 120 mm × 13 mm × 3.2 mm. The FTT cone calorimeter (UK) was applied to investigate the burning beheviours of PLA specimens (size: 100 mm × 100 mm × 3.0 mm) at a flux of 35 kW/m^2. Raman spectroscopy was undertaken on a DXR laser Raman spectrometer (Thermo Fisher, USA) under 532 nm laser excitation. X-ray photoelectron spectroscopy (XPS) was undertaken by an ESCALAB XI + apparatus (Thermo Fisher, USA) with Al Ka radiation source. Thermogravimetric-infrared spectroscopy (TG-IR) was undertaken by a TGA2 equipment (METTLER TOLEDO, Switzerland) linked to a TENSOR II facility (BRUKER, Germany), and the testing condition was the same as that of the above TGA test.

3. Results and discussion

3.1. Interphase reaction

As shown in Fig. 1a, during melt blending, PLA with terminal carboxyl group firstly reacted with ESO containing epoxy group to generate an intermediate (PLA/E), and then the residual epoxy group in the PLA/E intermediate reacted with the P–H group in DOPO to form the final PLA/xE/xD bioplastic. The torque variation of PLA and PLA/10E/3D during melt-blending is displayed in Fig. 1b. The sudden increase in the PLA torque curve was due to the addition of the PLA pellets, and then the torque gradually decreased and tended to equilibrium, indicating that the complete melting of the PLA particles. In the PLA/10E/3D torque variation curve, the addition of ESO and PLA also led to the increased torque. After that, the torque decreased significantly due to the system viscosity reduction. Then, the grafting reaction between PLA and ESO led to a sudden increase in torque. After the addition of DOPO, the torque fluctuated slightly, which was probably because of the ring-

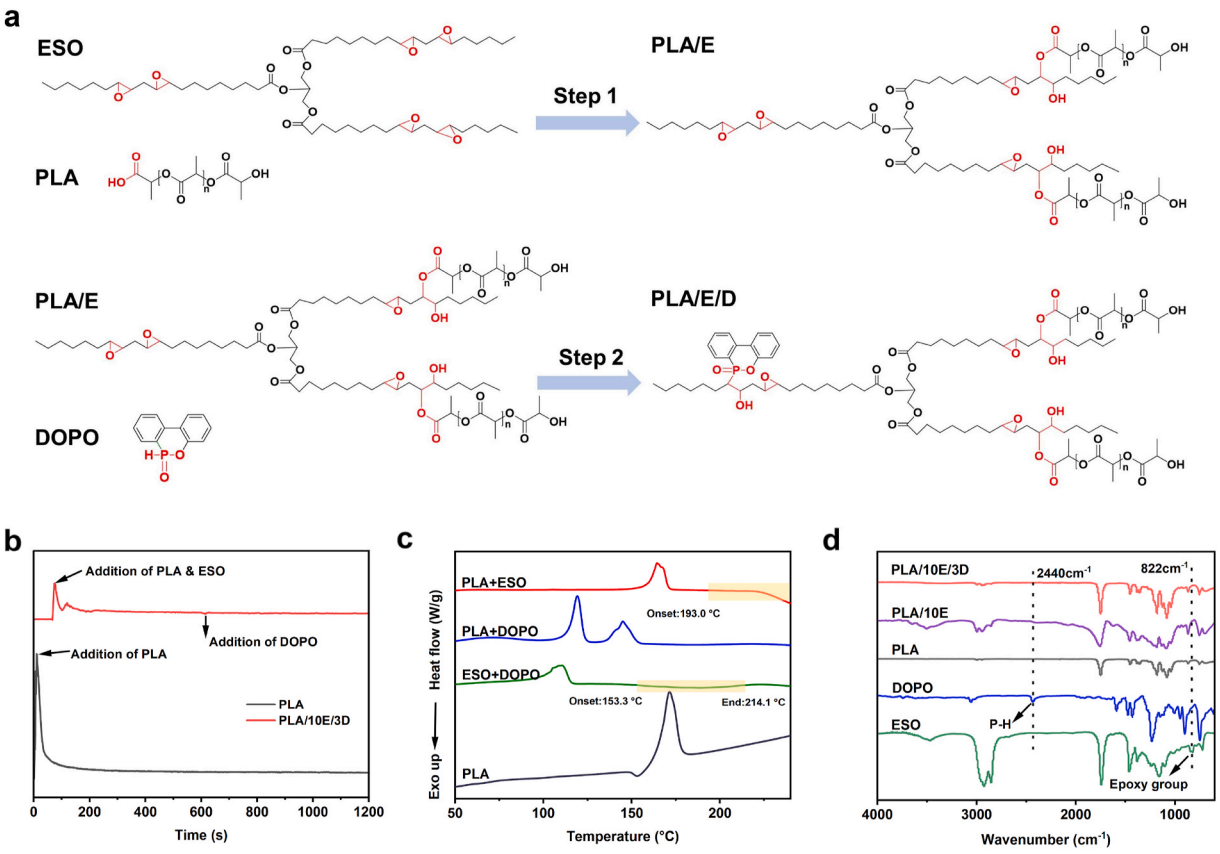

Fig. 1. (a) Illustration of the possible grafting reaction between PLA, ESO, and DOPO during melt-blending, (b) torque variation of PLA and PLA/10E/3D, (c) DSC diagrams of PLA, ESO + DOPO, PLA + DOPO and PLA + ESO, and (d) FTIR spectra of ESO, DOPO, PLA, PLA/10E, and PLA/10E/3D.

opening reaction between DOPO and ESO. Thus, the torque variation of PLA/10E/3D confirms its interphase reaction during melt-blending. According to previous work, ESO can react with PLA at about 200 °C [29]. The DSC curves of PLA, ESO + DOPO (mass ratio = 1:1), PLA + DOPO (mass ratio = 1:1), and PLA + ESO (mass ratio = 1:1) are shown in Fig. 1c and S1. Both PLA and PLA + DOPO only show endothermic melting peaks, indicating that there is no reaction between PLA and DOPO. In the DSC plot of PLA + DOPO, the first endothermic peak at about 120 °C is assigned to the melting of DOPO, and the second one at ~150 °C belongs to the fusion of PLA. Due to the catalytic decomposition effect of DOPO, mixing with it causes PLA to melt prematurely. PLA + ESO shows an exothermic peak in its DSC diagram, of which the onset temperature is approximately 193 °C, verifying that PLA can react with ESO during melt-blending (see Fig. S1). A similar phenomenon can be found in the DSC diagram of ESO + DOPO (see Fig. S1). Thus, PLA, ESO, and DOPO undergo the *in-situ* grafting exothermic reaction during the melt-blending process. The FTIR spectra of PLA, ESO, DOPO, PLA/10E, and PLA/10E/3D are presented in Fig. 1d. The characteristic absorption peak at 2440 cm^{-1} in the FTIR spectrum of DOPO belongs to the P–H bond, and that at 822 cm^{-1} of ESO is corresponded to the epoxy group [30]. Obviously, the absorption peak of the P–H bond completely disappears in the FTIR spectrum of PLA/10E/3D. For both PLA/10E and PLA/10E/3D, the peak intensity of the epoxy group is significantly reduced compared with ESO. In addition, the ^1H NMR spectra of PLA, ESO, PLA/E and PLA/E/D are shown in Fig. S2. The H-3, H-4, H-6, and H-8 peaks of ESO appear in the ^1H NMR of PLA/E, and both newly formed H-7′ and H-10 peaks also appear in the ^1H NMR of PLA/E, indicating the ring-opening reaction of ESO and PLA. All these results further confirm that both ESO and DOPO covalently link to the PLA chains during melt-blending by the reactions between the terminal carboxyl group of PLA, epoxy group of ESO and P–H group of DOPO.

3.2. Mechanical performances

The mechanical properties of PLA samples were characterized in detail, as shown in Fig. 2a–e and Table S1. The tensile strength and elongation at break of PLA are 67.9 MPa and 3.9 % (see Fig. 2a–c and Table S1), respectively, showing high mechanical strength but poor toughness. Grafting with ESO and DOPO significantly enhances the toughness of PLA/xE/xD composites and maintains high strength (see Fig. 2d). Among PLA/xE/xD composites, the PLA/10E/3D sample shows the highest elongation at break reaching 106.3 %, which is increased by 26.3 times relative to that of PLA. In addition, the tensile strength of the PLA/10E/3D sample is 52.8 MPa. Notably, both tensile strength and elongation at break of the PLA/10E/3D sample are much higher than those of PLA/10E and PLA/3D. This may be because ESO as a bio-plasticizer enhances the toughness, and DOPO as a rigid flame retardant improves the robustness. The enhanced toughness of PLA/xE/xD can also be confirmed by the increased impact strength, as shown in Fig. 2e. Specifically, the impact strength of PLA/15E/3D is 8.1 kJ/m^2, which is 102.5 % higher than 4.0 kJ/m^2 of PLA. To further evaluate the toughness of our PLA/10E/3D (passing a UL-94 V-0 rating, see 'Flame retardancy' section), its elongation at break and impact strength are compared with those of previous flame-retardant PLA with a UL-94 V-0 rating in Fig. 2f and Table S2 [6,12,15,29,31–38]. Obviously, our PLA/10E/3D exhibits much higher elongation at break and impact strength than previously reported flame-retardant PLA systems. Considering the superior toughness and simple reactive blending process, our PLA/10E/3D outperforms its counterparts.

The toughening mechanism of PLA/xE/xD was investigated by SEM and EDX, with the results shown in Fig. 2g–l and Table S3. The cross-section of PLA obtained from the notched Izod impact test is smooth with many regular stripes. However, both PLA/7.5E/3D and PLA/10E/

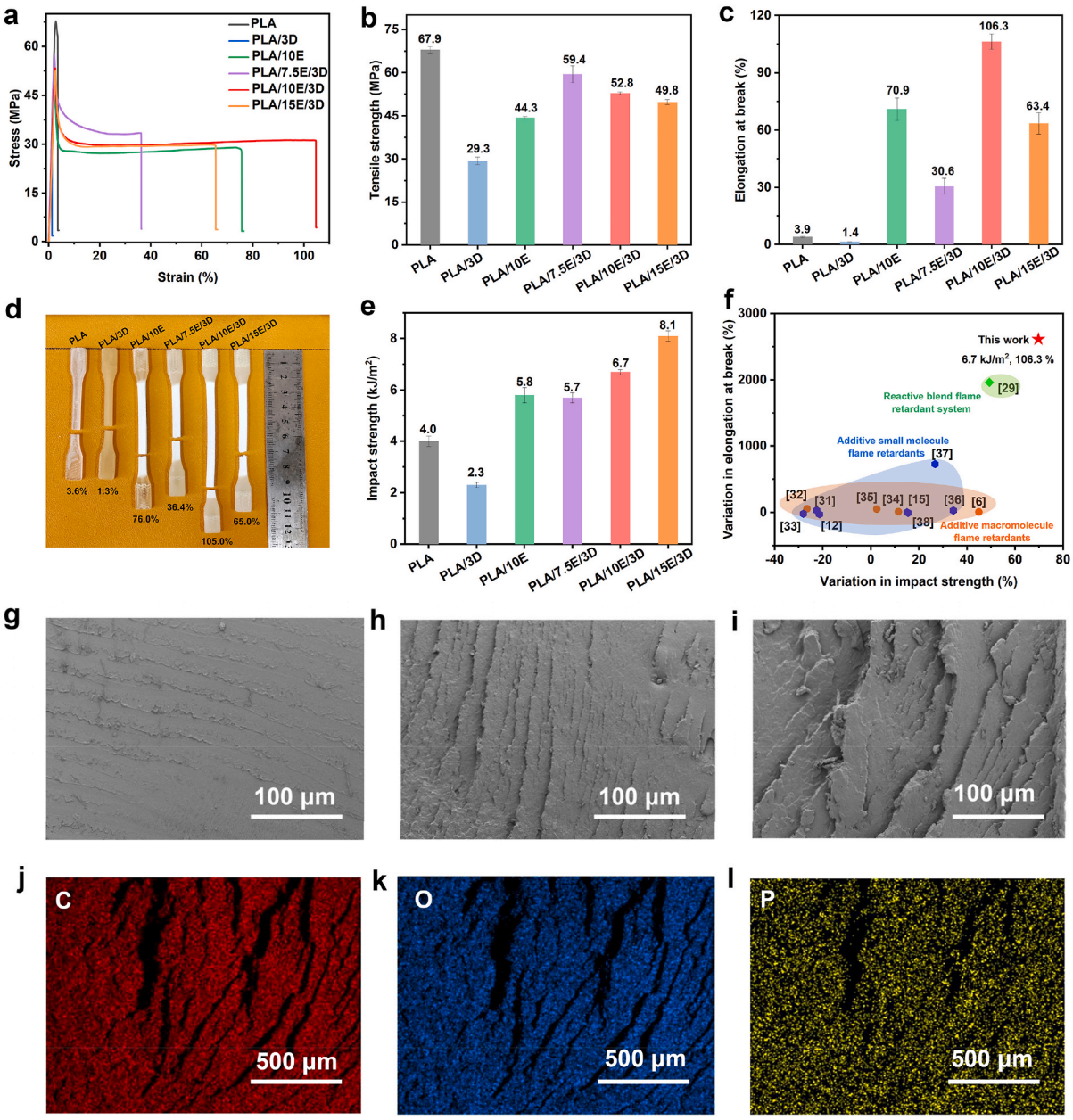

Fig. 2. (a) Tensile stress *vs*. strain plots of PLA and its composites, (b) tensile strength, and (c) elongation at break of PLA samples, (d) digital image of PLA samples after tensile failure, (e) impact strength of PLA samples, (f) elongation at break and impact strength of PLA/10E/3D and previous flame-retardant PLA with an UL-94 V-0 classification, SEM photographs of cross-sections for (g) PLA, (h) PLA/7.5E/3D, and (i) PLA/10E/3D after the notched Izod impact tests, and elemental mapping images of cross-section for PLA/10E/3D, (j) carbon, (k) oxygen, and (l) phosphorus.

3D exhibit wrinkled fracture surfaces, with obvious shear bands and microcracks. The formation of such a wrinkled cross-section under the action of external forces contributes to energy dissipation, bringing about enhanced toughness. Meanwhile, the elemental mapping photos of PLA/10E/3D in Fig. 2j–l confirm that the C, O, and P elements evenly distribute within the fracture surface. Thus, the *in-situ* grafting reaction between PLA, ESO, and DOPO enables the PLA/10E/3D bioplastic to form a homogeneous polymer system, which is critical for toughness enhancement. When subjected to external forces, the ESO part within PLA/10E/3D will induce plastic deformation of the matrix, manifested as the generation of shear bands and microcracks, ultimately consuming the fracture energy and thus improving toughness [39–41].

3.3. Thermal stability

The thermal stability of PLA samples under nitrogen atmosphere was evaluated by TGA. The thermogravimetric (TG) and derivative thermogravimetric (DTG) diagrams are shown in Fig. 3a and b. All DTG diagrams show only one peak, indicating that the PLA samples undergo a single thermal decomposition stage. As shown in Table 2, the temperature at 5 % mass loss ($T_{5\%}$) of PLA is 314.2 °C, while those of PLA/xE/xD samples are also around 314.0 °C, indicating that covalently grafting with ESO and DOPO does not damage the thermal stability of the PLA matrix. The heat-resistance index (T_{HRI}) values of PLA/xE/xD are also close to that of PLA, further indicative of their comparable thermal stability. Generally, the phosphorus-containing flame retardants will catalyze the decomposition of the PLA matrix during the melt-blending process, resulting in poor thermal stability [42,43]. In this

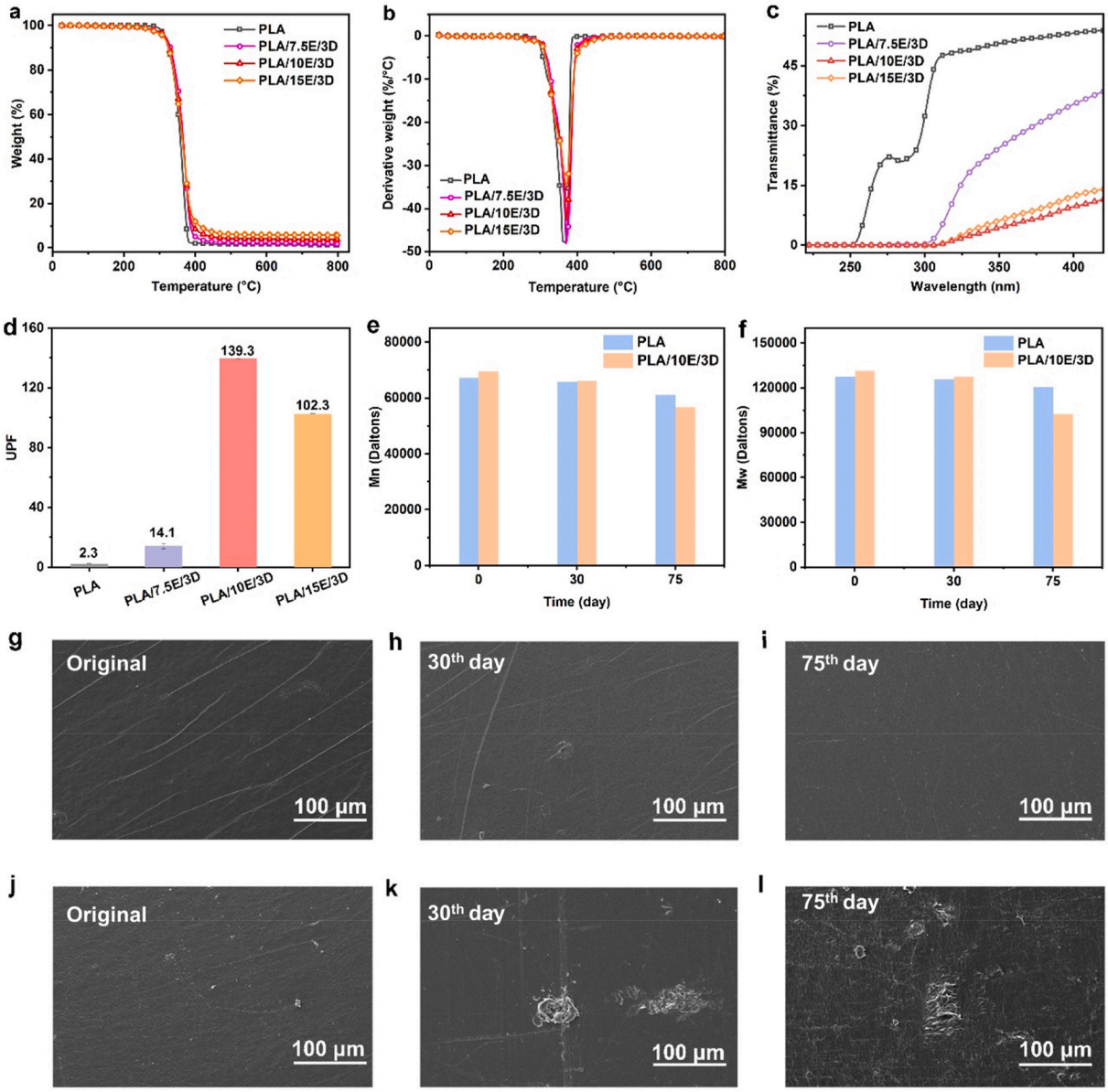

Fig. 3. (a) TG and (b) DTG plots of PLA samples in N_2 condition, (c) the UV–vis transmittance curves, and (d) ultraviolet protection factor (UPF) values of PLA samples, (e) M_n and (f) M_w of PLA and PLA/10E/3D samples after being buried in soil for different periods of time, and the SEM images of (g–i) PLA and (j–l) PLA/10E/3D samples after being buried in soil for different periods of time.

Table 2
TGA data of PLA and PLA composites.

Sample	$T_{5\%}$ (°C)	$T_{30\ \%}$ [a] (°C)	T_{max} (°C)	Y_c (%)	T_{HRI} [a] (°C)
PLA	314.2	346.9	366.3	1.22	163.6
PLA/7.5E/3D	316.1	352.7	370.8	1.70	165.6
PLA/10E/3D	314.2	350.8	372.4	3.79	164.7
PLA/15E/3D	310.3	348.9	372.2	5.79	163.4

[a] $T_{30\ \%}$: temperature at 30 % weight loss; and T_{HRI}: heat-resistance index, $T_{HRI} = 0.49 \times [T_{5\%}+0.6 \times (T_{30\%}-T_{5\%})]$.

work, the DOPO content is low, and ESO promotes the uniform dispersion of DOPO in the PLA matrix and produces grafting reactions, thus counteracting the negative effects of DOPO, so effectively maintaining thermal stability. In addition, the temperature at maximum weight loss rate (T_{max}) and char yield at 800 °C (Y_c) are both increased for PLA/xE/xD samples compared to PLA, demonstrating that introducing ESO and DOPO allows PLA to achieve enhanced high-temperature stability and char-formation performances. Hence, the PLA/xE/xD samples maintain their thermal stability and promote carbonization capabilities compared to PLA.

3.4. UV-shielding properties

The UV resistance of PLA films (thickness: ~0.2 mm) was investigated by UV spectrophotometer, with the UV plots presented in Fig. 3c. PLA shows high transmittance in the UV-B (280–320 nm) and UV-A (320–400 nm) ranges [44], indicating poor UV resistance. By contrast, the PLA/xE/xD bioplastic exhibits improved UV-shielding properties, in particular the transmittance of PLA/10E/3D is reduced to approximately 0 % in the UV-B range. At lower wavelengths (220–320 nm), PLA/xE/xD samples exhibit similar UV resistance due to their close DOPO content. As the wavelength increases (320–400 nm), the UV light is more easily transmitted through the PLA/xE/xD samples. Due to the low content of ESO, there is a small amount of DOPO in PLA/7.5E/3D samples does not reactive with ESO and thus tends to aggregate, which

affects the UV resistance at 320–400 nm. By further increasing the ESO content, DOPO can be fully reacted, resulting in enhanced and similar UV resistance properties for PLA/10E/3D and PLA/15E/3D. The ultraviolet protection factor (UPF) values of PLA samples are listed in Fig. 3d, in which the UPF value of PLA/10E/3D is up to 139.3 and ~60.0 times higher than 2.3 of PLA. It further confirms the enhanced UV resistance of PLA/10E/3D relative to PLA. The UV-blocking ability of biphenyl group from DOPO is responsible for the enhanced UV resistance of PLA/xE/xD samples [45]. Therefore, the PLA/xE/xD system with enhanced UV resistance is expected to be widely used in outdoor scenes.

3.5. Soil degradability

Due to its biodegradability and environmental friendliness, PLA has become the most commercialized bioplastic [46]. Unfortunately, the soil degradability of PLA is relatively slow [47,48]. According to previous work, the addition of some plasticizers can increase the degradation rate of PLA in soil [49]. To investigate the effects of ESO and DOPO on the soil degradation of PLA, soil burial experiments were conducted on both PLA and PLA/10E/3D specimens, and their structure and molecular weight variations after different time of burial were studied by GPC and SEM techniques (see Fig. 3e–l and Table S4). As shown in Fig. 3e and f, both weight average molecular weight (M_w) and number average molecular weight (M_n) of PLA and PLA/10E/3D are decreased with increasing burial time. Notably, the M_w and M_n of PLA/10E/3D are much lower than those of PLA on the 75th day, indicative of the enhanced soil degradation. Obviously, the introduction of ESO promotes the degradation of the PLA matrix when it is buried in soil. The enhanced soil degradation of PLA/10E/3D can also be confirmed by the SEM images in Fig. 3g–l. As presented in Fig. 3g–i, PLA maintains its smooth surface even after being buried for 75 days. However, the PLA/10E/3D surface becomes rough, and some cracks can be detected within the surface after being buried for 75 days (see Fig. 3j–l). Such a result further demonstrates the improved soil degradation of PLA/10E/3D relative to PLA. Hence, reactive blending with ESO and DOPO can also enhance the biodegradation of PLA, which promotes sustainable development.

3.6. Flame retardancy

The LOI values and UL-94 classifications of PLA samples are listed in Fig. 4a and Table 3. PLA is a highly flammable material, reflected in its low LOI of 19.5 % and severe dripping and violent combustion in UL-94 testing. With the addition of 3 wt% DOPO, the PLA/3D sample achieves the UL-94 V-0 rating, and its LOI is increased to 26.0 %, indicative of the high flame-retardant efficiency of DOPO. However, the PLA/3D sample suffers from poor mechanical properties (See Table S1) because of the catalytic degradation effect of DOPO, which significantly restricts its practical application. Introducing ESO cannot enhance the flame retardancy of PLA, and thus the LOI of the PLA/10E sample is only 19 %, and it cannot achieve any rating in the UL-94 test. When simultaneously incorporating ESO and DOPO, all PLA/xE/xD samples pass the UL-94 V-0 rating, and their LOI values range from 26.2% to 29.4 %, which are higher than those of PLA, PLA/3D, and PLA/10E samples. The P–H group of DOPO in PLA/3D will catalyze the decomposition of PLA, which affects the LOI value. In PLA/7.5E/3D, ESO consumes the P–H group of DOPO by ring-opening reaction, which avoids the PLA matrix degradation caused by the introduction of DOPO. Hence, the LOI of PLA/7.5E/3D is higher than that of PLA/3D. When ESO content is gradually increased, there will be some unreacted ESO molecules remained in the PLA matrix. ESO, as a flammable chemical, will lower the LOI of PLA/E/D. In conclusion, LOI decreases gradually with increasing ESO content, and the PLA/15E/3D has the lowest LOI value. Thus, reactive blending with ESO and DOPO not only effectively enhances the toughness of PLA, but also endows it with improved flame retardancy.

Table 3
LOI and UL-94 results of PLA samples.

Sample	LOI (%)	UL-94 (3.2 mm)			
		av-(t_1+ t_2) (s)	Dripping	Cotton ignition	Rating
PLA	19.5	>50	Yes	Yes	NR
PLA/3D	26.0	4.3	Yes	No	V-0
PLA/10E	19.0	>50	Yes	Yes	NR
PLA/7.5E/3D	29.4	1.8	Yes	No	V-0
PLA/10E/3D	27.5	4.1	Yes	No	V-0
PLA/15E/3D	26.2	5.1	Yes	No	V-0

The cone calorimetry is the most representative test method to evaluate the combustion behaviors of materials in a real fire environment, and the corresponding results of PLA and PLA/xE/xD samples are shown in Table S5 and Fig. 4b and c. The time to ignition (TTI) values of three PLA/xE/xD samples are about 60 s, which are comparable to that of PLA, which is consistent with the TGA result. All PLA/xE/xD samples show reduced peak heat release rate (PHRR) and total heat release

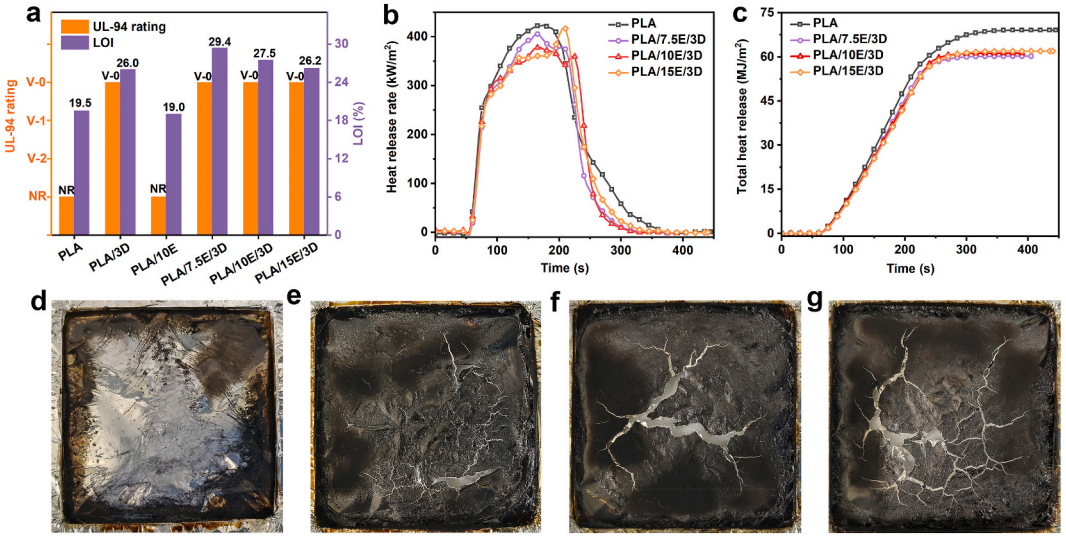

Fig. 4. (a) UL-94 ratings and LOI values of PLA samples, (b) heat release rate and (c) total heat release of PLA samples, and digital photographs of (d) PLA, (e) PLA/7.5E/3D, (f) PLA/10E/3D, and (g) PLA/15E/3D chars after cone calorimetry test.

(THR) compared with those of PLA. The PHRR and THR of PLA are 426.7 kW/m^2 and 69.1 MJ/m^2, while those of PLA/10E/3D are 380.2 kW/m^2 and 61.3 MJ/m^2, with 10.9 % and 11.3 % reductions. Moreover, the PLA/10E/3D sample displays lower average effective combustion heat (AEHC), and higher average carbon monoxide yield (ACOY) than PLA. The average carbon dioxide yield (ACO_2Y) of PLA/10E/3D is lower than that of PLA. The results demonstrate that the gas-phase combustion degree of PLA/10E/3D is lower than that of PLA, which is mainly due to the quenching radical effect of DOPO. The char yield at 500 s (CY) of PLA/10E/3D is 5 times higher than that of PLA, indicative of its condensed-phase flame retardancy. Obviously, PLA/10E/3D feature significantly enhanced flame retardancy due to its reduced gas-phase burning degree and enhanced char-forming ability.

3.7. Char residue analysis

The condensed-phase flame-retardant mechanism of PLA/xE/xD was first studied by the Raman technique, with the spectra shown in Fig. 5a. In the spectra, the D peak represents the disordered carbon structure, and the G one represents the ordered carbon structure, and the area ratio of D peak to G peak (I_D/I_G) is inversely proportional to the char graphitization degree [30,50]. The I_D/I_G value of the PLA char is as high as 5.77, while the PLA/xE/xD chars show much lower I_D/I_G values, which are approximately 3.0. The unreacted small-molecule ESOs are more susceptible to thermal decomposition, leading to a monotonic increase in the I_D/I_G of PLA/xE/xD with increasing ESO, which is consistent with the results of LOI testing. The results show that the P element in DOPO catalyzes the formation of a dense char layer. The char layers can not only prevent the diffusion of pyrolyzed volatiles but also isolate the thermal and oxygen exchange in the combustion process [51–53].

The elemental contents and bonding states of PLA and PLA/10E/3D chars were studied by XPS in Fig. 5b–f and S3 and Table S6. The C and O elements can be found in the char of PLA (see Fig. 5b and S3), and the C, O and P elements can be detected in the residue of PLA/10E/3D (see Fig. 5c). In the C1s spectrum of PLA/10E/3D char, the peaks at 287.5, 285.9 and 284.3 eV are attributed to the C═O, C–O–P, and C–H/C structures, respectively (see Fig. 5d). In the O1s XPS spectrum of PLA/10E/3D char, the peaks at 533.8, 533.1 and 531.1 eV are assigned to the C–OH, C–O/P and C═O/P bonds, respectively (see Fig. 5e). In the P2p XPS spectrum of PLA/10E/3D char, the peaks at 134.1 and 133.8 eV belong to the P–C and P═O bonds, respectively [36,54]. In addition, according to the XPS results of the PLA/10E/3D char, the phosphorus content is 2.04 wt% (see Table S6), which also indicates that DOPO plays an important role in the char formation in the condensed phase. These results confirm that the pyrolysis products of DOPO participate in the char-forming reaction of the PLA matrix in the combustion procedure, thus improving the flame retardancy of PLA/10E/3D.

3.8. TG-IR analysis

The TG-IR test of PLA and PLA/10E/3D was conducted in a nitrogen atmosphere, with the spectra shown in Fig. 6a–f. The gaseous products of PLA and PLA/10E/3D samples are identical in the TG-IR tests (see Fig. 6a–e), including water (3576 cm^{-1}), hydrocarbons (2732 and 1370 cm^{-1}), CO_2 (2356 cm^{-1}), CO (2170 cm^{-1}), carbonyl compounds (1762 cm^{-1}), fragments with C–O group (1238 cm^{-1}), and aliphatic ester (1100 cm^{-1}) [55–57]. Compared with PLA, PLA/10E/3D shows lower intensities of these absorption peaks (see Fig. 6c and f), indicating that DOPO suppresses the thermal decomposition of PLA. Generally, the phosphorus-containing fragments of DOPO capture the active radicals, thus reducing the degree of gas-phase combustion [52]. Due to the low phosphorus content, it is hard to detect the phosphorus-based fragments during the TG-IR test of PLA/10E/3D. However, according to the AEHC results, DOPO effectively suppresses the gas-phase combustion degree of PLA composite. In summary, the P-containing decomposition products of DOPO catalyze the PLA composite to form a dense and foamed char with a high degree of graphitization on its surface during combustion, which can inhibit heat transfer and protect the underlying substrate. Meanwhile, the phosphorus-based radicals derived from DOPO trap the active radicals generated by the degradation of the PLA composite, thereby inhibiting combustion in the gas phase. Therefore, the outstanding flame retardancy of PLA/xE/xD is mainly due to the bi-phase action of DOPO.

4. Conclusions

By simple reactive blending of PLA, ESO, and DOPO, flame-retardant, tough, and strong PLA/xE/xD bioplastics with enhanced UV

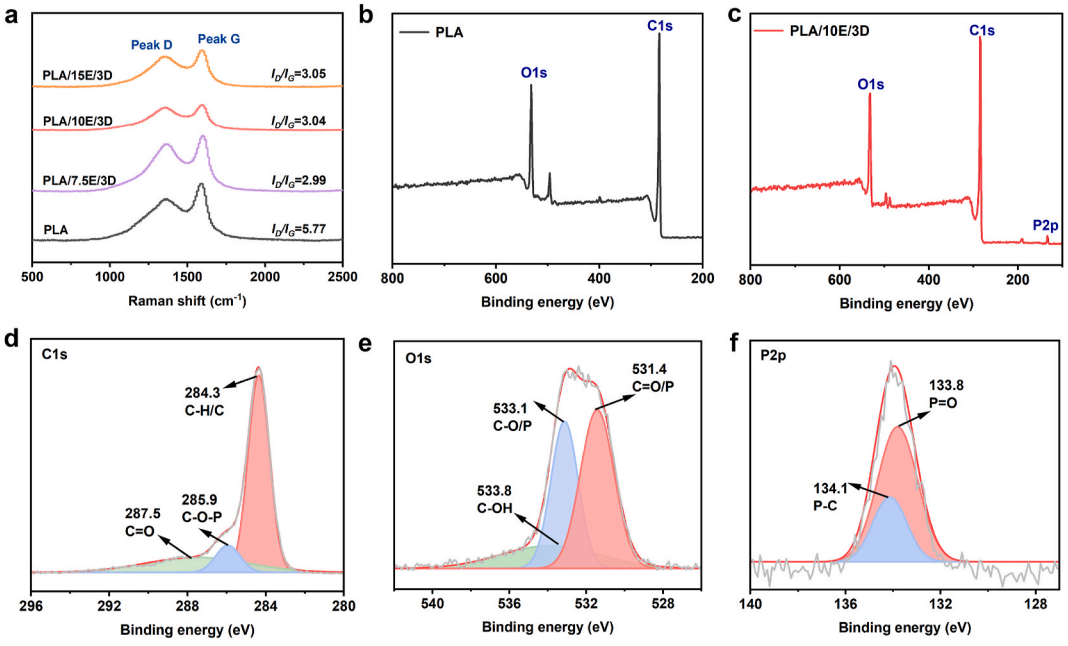

Fig. 5. (a) Raman spectra of the residual chars for PLA, PLA/7.5E/3D, PLA/10E/3D, and PLA/15E/3D after cone calorimetry, XPS full-scan spectra of (b) PLA, and (c) PLA/10E/3D chars, and high-resolution (g) C1s, (h) O1s, and (i) P2p spectra of PLA/10E/3D residues.

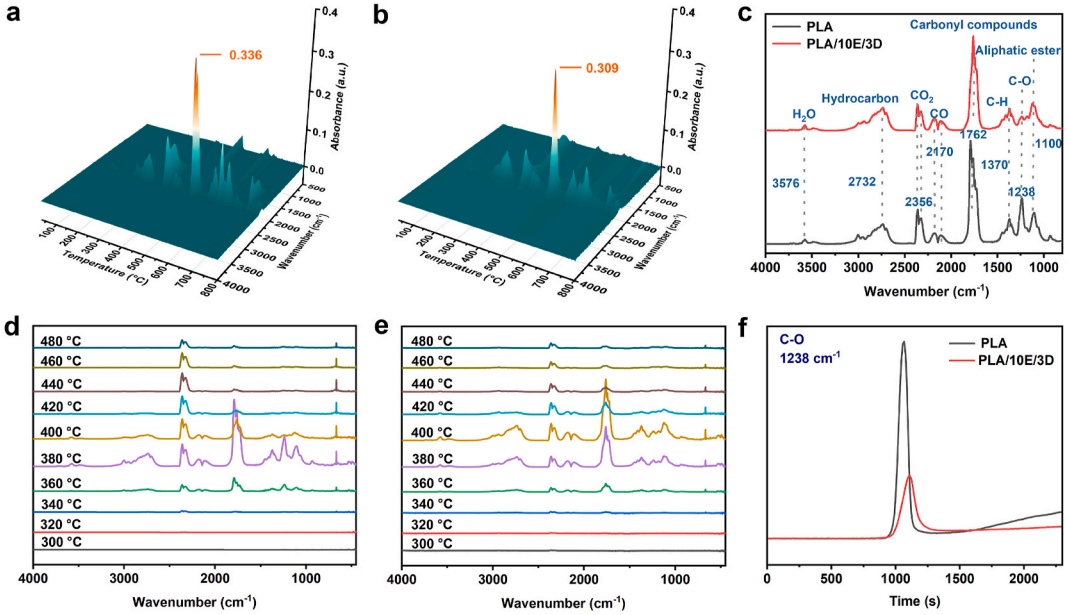

Fig. 6. 3D IR spectra of (a) PLA and (b) PLA/10E/3D decomposition products, (c) IR spectra of PLA and PLA/10E/3D decomposition products at T_{max}, IR spectra of (d) PLA and (e) PLA/10E/3D decomposition products at different temperatures, and the absorption *vs.* time curves of the peak at 1238 cm^{-1} of PLA and PLA/10E/3D samples.

resistance, soil degradation, and great thermal stability were fabricated in this work. PLA/10E/3D with 10 wt% of ESO and 3.0 wt% of DOPO displays a tensile strength of 52.8 MPa, and its elongation at break and impact strength reach 106.3 % and 6.7 kJ/m^2, which increase by 26.3 times and 67.5 % relative to those of PLA. It demonstrates that PLA/10E/3D features superior toughness and well-preserved mechanical strength due to the introduction of ESO and DOPO. In addition, the thermal stability (T_{HRI} = 164.7 °C) of PLA/10E/3D bioplastic is comparable to that of PLA, and its char-forming ability (Y_c = 3.79 %) and UV resistance (UPF = 139.3) are significantly enhanced. Notably, PLA/10E/3D achieves an UL-94 V-0 rating with a LOI of 27.5 %, indicative of its great flame retardancy. The effects of ESO and DOPO on the soil degradation of PLA was also explored, and the results showed that ESO and DOPO could accelerate the degradation rate of PLA in soil. Thereby, this work provides a simple and green approach for the fabrication of toughened, UV/heat-resistant, and flame-retardant PLA composites with improved soil degradation ability, which will promote the development of high-performance bioplastics.

CRediT authorship contribution statement

Zimeng Zhang: Writing – original draft, Investigation, Data curation. **Siqi Huo:** Writing – review & editing, Supervision, Project administration, Conceptualization. **Guofeng Ye:** Formal analysis. **Cheng Wang:** Methodology. **Qi Zhang:** Supervision. **Zhitian Liu:** Supervision, Project administration.

Declaration of competing interest

The authors declare that they have no known competing financial interests or personal relationships that could have appeared to influence the work reported in this paper.

Data availability

Data will be made available on request.

Acknowledgments

This work was funded by the Australian Research Council (DE230100616).

Appendix A. Supplementary data

Supplementary data to this article can be found online at https://doi.org/10.1016/j.mtchem.2024.102252.

References

[1] K. Cai, X. Wang, C. Yu, J. Zhang, S. Tu, J. Feng, Enhancing the mechanical properties of PBAT/thermoplastic starch (TPS) biodegradable composite films through a dynamic vulcanization process, ACS Sustain. Chem. Eng. 12 (4) (2024) 1573–1583, https://doi.org/10.1021/acssuschemeng.3c06847.
[2] W. Pang, B. Li, Y. Wu, Q. Zeng, J. Yang, Y. Zhang, S. Tian, Upgraded recycling of biodegradable PBAT plastic: efficient hydrolysis and electrocatalytic conversion, Chem. Eng. J. 486 (2024) 150342, https://doi.org/10.1016/j.cej.2024.150342.
[3] S. Nara, K. Su Hyun, O. Jinok, K. Suwon, L. Yeda, S. Yuni, C. Suhye, B. Shashi Kant, K. Yun-Gon, Y. Yung-Hun, Reproducible polybutylene succinate (PBS)-degrading artificial consortia by introducing the least type of PBS-degrading strains, Polymers 16 (5) (2024) 651, https://doi.org/10.3390/polym16050651.
[4] Q. Qin, Y. Yang, C. Yang, L. Zhang, H. Yin, F. Yu, J. Ma, Degradation and adsorption behavior of biodegradable plastic PLA under conventional weathering conditions, Sci. Total Environ. 842 (2022) 156775, https://doi.org/10.1016/j.scitotenv.2022.156775.
[5] K. Jee Young, K. Ka Young, J. Woo Shik, K. Hyun Soo, O. Byeolnim, P. Jaewon, E. C. Yoon, Effects of micro-sized biodegradable plastics on microcystis aeruginosa, Sci. Total Environ. 912 (2023) 169044, https://doi.org/10.1016/j.scitotenv.2023.169044.
[6] Y. Yu, C. Ma, H. Zhang, Y. Zhang, Z. Fang, R. Song, Z. Lin, J. Feng, P. Song, Combination effects of a bio-based fire retardant and functionalized graphene oxide on a fire retardant and mechanical properties of polylactide, Mater. Today Chem. 30 (2023) 101565, https://doi.org/10.1016/j.mtchem.2023.101565.
[7] D. Shuangshuang, W. Xuehui, W. Zhigang, Supertoughened polylactide via the addition of low content poly(ε-caprolactone) and tensile deformation above the glass transition temperature, Macromolecules 56 (13) (2023) 5089–5100, https://doi.org/10.1021/acs.macromol.3c00195t.
[8] L. Yuanyuan, D. Qiang, Improving the compatibility and toughness of sustainable polylactide/poly(butylene adipate-co-terephthalate) blends by incorporation of peroxide and diacrylate, Int. J. Biol. Macromol. 259 (2024) 129355, https://doi.org/10.1016/j.ijbiomac.2024.129355.
[9] R. Yang, N. Li, C.J. Evans, S. Yang, K. Zhang, Phosphaphenanthrene-functionalized benzoxazines bearing intramolecularly hydrogen-bonded phenolic hydroxyl: synthesis, structural characterization, polymerization mechanism, and property

investigation, Macromolecules 56 (4) (2023) 1311–1323, https://doi.org/10.1021/acs.macromol.3c00028.
[10] J. Yang, X. Song, X. Chen, Y. Wang, J. Shi, Z. Zheng, H. Xu, L. Liu, A soluble salen-DOPO flame retardant for efficiently improving PBAT/PLLA film, Chem. Eng. J. 476 (2023) 146669, https://doi.org/10.1016/j.cej.2023.146669.
[11] C. Yargici Kovanci, M. Nofar, A. Ghanbari, Synergistic enhancement of flame retardancy behavior of glass-fiber reinforced polylactide composites through using phosphorus-based flame retardants and chain modifiers, Polymers 14 (23) (2022) 5324, https://doi.org/10.3390/polym14235324.
[12] X. Ma, N. Wu, P. Liu, H. Cui, Fabrication of highly efficient phenylphosphorylated chitosan bio-based flame retardants for flammable PLA biomaterial, Carbohydr. Polym. 287 (2022) 119317, https://doi.org/10.1016/j.carbpol.2022.119317.
[13] M. Ma, X. Wang, K. Liu, S. Chen, Y. Shi, H. He, X. Wang, Achieving simultaneously toughening and flame-retardant modification of poly(lactic acid) by in-situ formed cross-linked polyurethane and reactive blending with ammonium polyphosphate, J. Mater. Sci. 57 (9) (2022) 5645–5657, https://doi.org/10.1007/s10853-022-06887-5.
[14] L. Liu, C. Yan, W. Zhang, Y. Xu, M. Xu, Y. Hong, Y. Qiu, B. Li, A monomolecular organophosphate for enhancing the flame retardancy, thermostability and crystallization properties of polylactic acid, J. Appl. Polym. Sci. 140 (4) (2022) e53347, https://doi.org/10.1002/app.53347.
[15] Y. Xue, Z. Ma, X. Xu, M. Shen, G. Huang, S. Bourbigot, X. Liu, P. Song, Mechanically robust and flame-retardant polylactide composites based on molecularly-engineered polyphosphoramides, Compos. Part. A-Appl. S. 144 (2021) 106317, https://doi.org/10.1016/j.compositesa.2021.106317.
[16] Y. Xiao, Y. Yang, Q. Luo, B. Tang, J. Guan, Q. Tian, Construction of carbon-based flame retardant composite with reinforced and toughened property and its application in polylactic acid, RSC Adv. 12 (34) (2022) 22236–22243, https://doi.org/10.1039/d2ra04130h.
[17] L. Xia, R.-k. Jian, Y.-f. Ai, X.-l. Zheng, B. Zhao, An effective multi-hydroxy-containing ammonium phosphate towards flame-retarding poly(lactic acid): flame retardance, thermal and pyrolysis behaviors, J. Anal. Appl. Pyrol. 134 (2018) 265–273, https://doi.org/10.1016/j.jaap.2018.06.016.
[18] N. Wu, J. Yu, W. Lang, X. Ma, Y. Yang, Flame retardancy and toughness of poly (lactic acid)/GNR/SiAHP composites, Polymers 11 (7) (2019) 1129, https://doi.org/10.3390/polym11071129.
[19] F. Wu, G.-Q. Tian, J.-W. Yang, J. Tan, Simultaneously improving the toughness and flame retardancy of poly(lactic acid) by incorporating a novel bifunctional macromolecular ionomer, Polymer 240 (2022) 124494, https://doi.org/10.1016/j.polymer.2021.124494.
[20] X. Wen, Z. Liu, Z. Li, J. Zhang, D.-Y. Wang, K. Szymańska, X. Chen, E. Mijowska, T. Tang, Constructing multifunctional nanofiller with reactive interface in PLA/CB-g-DOPO composites for simultaneously improving flame retardancy, electrical conductivity and mechanical properties, Compos. Sci. Technol. 188 (2020) 107988, https://doi.org/10.1016/j.compscitech.2019.107988.
[21] X. Chen, R. Zhang, Y. Mao, L. Zhong, P. Lin, Q. Deng, B. Zheng, H. Shen, Z. Feng, H. Zhang, Development of a toughened and antibacterial poly(lactide acid) (PLA) with preserved strength by elemental sulfur-based bio-renewable dynamically crosslinked elastomers, Chem. Eng. J. 467 (2023) 143419, https://doi.org/10.1016/j.cej.2023.143419.
[22] D. Han, H. Wang, T. Lu, L. Cao, Y. Dai, H. Cao, X. Yu, Scalable manufacturing green ccore-shell structure flame retardant, with enhanced mechanical and flame-retardant performances of polylactic acid, J. Polym. Environ. 30 (6) (2022) 2516–2533, https://doi.org/10.1007/s10924-021-02358-1.
[23] X. Song, C. Zhang, Y. Yang, Y. Weng, Effect of oligomers from epoxidized soybean oil and sebacic acid on the toughness of polylactic acid/bamboo fiber composites, J. Appl. Polym. Sci. 139 (5) (2021) 51583, https://doi.org/10.1002/app.51583.
[24] S. Mahmud, Y. Long, M. Abu Taher, Z. Xiong, R. Zhang, J. Zhu, Toughening polylactide by direct blending of cellulose nanocrystals and epoxidized soybean oil, J. Appl. Polym. Sci. 136 (46) (2019) 48221, https://doi.org/10.1002/app.48221.
[25] Y.-B. Liu, Z. Xu, Z.-M. Zhang, R.-Y. Bao, M.-B. Yang, W. Yang, Blowing tough polylactide film enabled by the in situ construction of covalent adaptive networks with epoxidized soybean oil as dynamic crosslinks, Green Chem. Eng. 25 (13) (2023) 5182–5194, https://doi.org/10.1039/d3gc00999h.
[26] W. Liu, J. Qiu, T. Chen, M. Fei, R. Qiu, E. Sakai, Regulating tannic acid-crosslinked epoxidized soybean oil oligomers for strengthening and toughening bamboo fibers-reinforced poly(lactic acid) biocomposites, Compos. Sci. Technol. 181 (2019) 107709, https://doi.org/10.1016/j.compscitech.2019.107709.
[27] T. Chen, Y. Wu, J. Qiu, M. Fei, R. Qiu, W. Liu, Interfacial compatibilization via in-situ polymerization of epoxidized soybean oil for bamboo fibers reinforced poly (lactic acid) biocomposites, Compos. Part. A-Appl. S. 138 (2020) 106066, https://doi.org/10.1016/j.compositesa.2020.106066.
[28] Q.-y. Ge, Q. Dou, Preparation of supertough polylactide/polybutylene succinate/epoxidized soybean oil bio-blends by chain extension, ACS Sustain. Chem. Eng. 11 (26) (2023) 9620–9629, https://doi.org/10.1021/acssuschemeng.3c01042.
[29] X. Xu, J. Dai, Z. Ma, L. Liu, X. Zhang, H. Liu, L.-C. Tang, G. Huang, H. Wang, P. Song, Manipulating interphase reactions for mechanically robust, flame-retardant and sustainable polylactide biocomposites, Compos. Part. B-Eng. 190 (2020) 107930, https://doi.org/10.1016/j.compositesb.2020.107930.
[30] Z. Chi, Z. Guo, Z. Xu, M. Zhang, M. Li, L. Shang, Y. Ao, A DOPO-based phosphorus-nitrogen flame retardant bio-based epoxy resin from diphenolic acid: synthesis, flame-retardant behavior and mechanism, Polym. Degrad. Stabil. 176 (2020) 109151, https://doi.org/10.1016/j.polymdegradstab.2020.109151.
[31] W. Yu, W. Yang, P. Xu, C. Dai, Q. Liu, P. Ma, Simultaneously enhance the fire safety and mechanical properties of PLA by incorporating a cyclophosphazene-based flame retardant, E-Polymers 22 (1) (2022) 411–429, https://doi.org/10.1515/epoly-2022-0041.
[32] Y. Chen, J. He, Z. Sun, B. Xu, J. Li, L. Qian, Grafting cellulose nanocrystals with phosphazene-containing compound for simultaneously enhancing the flame retardancy and mechanical properties of polylactic acid, Cellulose 29 (2021) 6143–6160, https://doi.org/10.21203/rs.3.rs-888411/v1.
[33] X. Wang, W. He, L. Long, S. Huang, S. Qin, G. Xu, A phosphorus- and nitrogen-containing DOPO derivative as flame retardant for polylactic acid (PLA), J. Therm. Anal. Calorim. 145 (2) (2020) 331–343, https://doi.org/10.1007/s10973-020-09688-7.
[34] L. Liu, M. Yao, H. Zhang, Y. Zhang, J. Feng, Z. Fang, P. Song, Aqueous self-assembly of bio-based flame retardants for fire-retardant, smoke-suppressive, and toughened polylactic acid, ACS Sustain. Chem. Eng. 10 (49) (2022) 16313–16323, https://doi.org/10.1021/acssuschemeng.2c05298.
[35] K. Olonisakin, R. Li, S. He, W. Aishi, F. Lifei, C. Mengting, Z. Xin-Xiang, J. Ruohai, W. Yang, Flame rating of nano clay/MCC/PLA composites with both reinforced strength and toughness, J. Polym. Res. 29 (12) (2022) 502, https://doi.org/10.1007/s10965-022-03351-5.
[36] L. Yu, S. Huo, C. Wang, G. Ye, P. Song, J. Feng, Z. Fang, H. Wang, Z. Liu, Flame-retardant poly(L-lactic acid) with enhanced UV protection and well-preserved mechanical properties by a furan-containing polyphosphoramide, Int. J. Biol. Macromol. 234 (2023) 123707, https://doi.org/10.1016/j.ijbiomac.2023.123707.
[37] J. Qi, Y. Pan, Z. Luo, B. Wang, Facile and scalable fabrication of bioderived flame retardant based on adenine for enhancing fire safety of fully biodegradable PLA/PBAT/TPS ternary blends, J. Appl. Ppolym. Sci. 138 (35) (2021) 50877, https://doi.org/10.1002/app.50877.
[38] H. Cheng, Y. Wu, W. Hsu, F. Lin, S. Wang, J. Zeng, Q. Zhu, L. Song, Green and economic flame retardant prepared by the one-step method for polylactic acid, Int. J. Biol. Macromol. 253 (2023) 127291, https://doi.org/10.1016/j.ijbiomac.2023.127291.
[39] R. Yang, C. Cai, X. Han, Z. Chen, G. Gu, C. Zhang, G. Zou, J. Li, Supertough and biodegradable poly(lactic acid) blends with “hard-soft” core-shell unsaturated poly (ether-ester) through self-vulcanization, Macromolecules 56 (18) (2023) 7271–7285, https://doi.org/10.1021/acs.macromol.3c01126.
[40] K. Xu, C. Yan, C. Du, Y. Xu, B. Li, L. Liu, Preparation and mechanism of toughened and flame-retardant bio-based polylactic acid composites, Polymers 15 (2) (2023) 300, https://doi.org/10.3390/polym15020300.
[41] C.-B. Sun, H.-D. Mao, F. Chen, Q. Fu, Preparation of polylactide composite with excellent flame retardance and improved mechanical properties, Chin. J. Polym. Sci. 36 (12) (2018) 1385–1393, https://doi.org/10.1007/s10118-018-2150-7.
[42] D.M. Bao, J.H. Wang, Z.M. Hou, Z.Y. Xu, X.L. Ye, Y.Z. Qi, S.J. Xu, L.J. Long, Z. L. Wu, Z. Wen, Synthesis of a novel flame retardant with phosphaphenanthrene and phosphazene double functional groups and flame retardancy of poly (lactic acid) composites, Front. Mater. 9 (2022) 951515, https://doi.org/10.3389/fmats.2022.951515.
[43] Y. Tan, D. Zhang, Y. Xue, X. Zhan, F. Tan, S. Qin, Flame retardant properties and mechanism of PLA/P-PPD -Ph/ECE conjugated flame retardant composites, Front. Chem. 11 (2023) 1096526, https://doi.org/10.3389/fchem.2023.1096526.
[44] W. Zhong, P. Xu, D. Niu, Q. Wang, W. Yang, X. Zhang, T. Liu, P. Ma, Enhanced flame retardancy, ultraviolet shielding, and preserved mechanical properties of polylactic acid with fully biobased multifunctional additives by a green method, ACS Sustain. Chem. Eng. 12 (10) (2024) 4017–4027, https://doi.org/10.1021/acssuschemeng.3c06993.
[45] Y. Zhang, J. Jing, T. Liu, L. Xi, T. Sai, S. Ran, Z. Fang, S. Huo, P. Song, A molecularly engineered bioderived polyphosphate for enhanced flame retardant, UV-blocking and mechanical properties of poly(lactic acid), Chem. Eng. J. 411 (2021) 128493, https://doi.org/10.1016/j.cej.2021.128493.
[46] Y. Li, S. Qiu, J. Sun, Y. Ren, S. Wang, X. Wang, W. Wang, H. Li, B. Fei, X. Gu, S. Zhang, A new strategy to prepare fully bio-based poly(lactic acid) composite with high flame retardancy, UV resistance, and rapid degradation in soil, Chem. Eng. J. 428 (2022) 131979, https://doi.org/10.1016/j.cej.2021.131979.
[47] Y. Boonluksiri, B. Prapagdee, N. Sombatsompop, Promotion of polylactic acid biodegradation by a combined addition of PLA-degrading bacterium and nitrogen source under submerged and soil burial conditions, Polym. Degrad. Sttabil. 188 (2021) 109562, https://doi.org/10.1016/j.polymdegradstab.2021.109562.
[48] S. Qiu, Y. Li, P. Qi, D. Meng, J. Sun, H. Li, Z. Cui, X. Gu, S. Zhang, Improving the flame retardancy and accelerating the degradation of poly (lactic acid) in soil by introducing fully bio-based additives, Int. J. Biol. Macromol. 193 (2021) 44–52, https://doi.org/10.1016/j.ijbiomac.2021.10.119.
[49] S. Sharma, A. Majumdar, B.S. Butola, Tailoring the biodegradability of polylactic acid (PLA) based films and ramie-PLA green composites by using selective additives, Int. J. Biol. Macromol. 181 (2021) 1092–1103, https://doi.org/10.1016/j.ijbiomac.2021.04.108.
[50] M. Yao, L. Liu, C. Ma, H. Zhang, Y. Zhang, R. Song, Z. Fang, P. Song, A lysine-derived flame retardant for improved flame retardancy, crystallinity, and aqueous-phase degradation of polylactide, Chem. Eng. J. 462 (2023) 142189, https://doi.org/10.1016/j.cej.2023.142189.
[51] Y. He, X. Cui, Z. Liu, F. Lan, J. Sun, H. Li, X. Gu, S. Zhang, A new approach to prepare flame retardant epoxy resin with excellent transmittance, mechanical properties, and anti-aging performance by the incorporation of DOPO derivative, Polym. Degrad. Stabil. 218 (2023) 110579, https://doi.org/10.1016/j.polymdegradstab.2023.110579.
[52] C. Wang, S. Huo, G. Ye, P. Song, H. Wang, Z. Liu, A P/Si-containing polyethylenimine curing agent towards transparent, durable fire-safe, mechanically-robust and tough epoxy resins, Chem. Eng. J. 451 (2022) 138768, https://doi.org/10.1016/j.cej.2022.138768.

[53] M. Bu, X. Zhang, T. Zhou, C. Lei, In-situ formation of polynanosiloxane by a multifunctional phosphaphenanthrene-silicone-epoxy soybean oil flame retardant improves the toughness and transparency of epoxy resin, ACS Appl. Polym. Mater. 6 (2024) 8056–8072, https://doi.org/10.1021/acsapm.4c00822.
[54] J. Zhang, X. Mi, S. Chen, Z. Xu, D. Zhang, M. Miao, J. Wang, A bio-based hyperbranched flame retardant for epoxy resins, Chem. Eng. J. 381 (2019) 122719, https://doi.org/10.1016/j.cej.2019.122719.
[55] Y.-W. Jia, X. Zhao, T. Fu, D.-F. Li, Y. Guo, X.-L. Wang, Y.-Z. Wang, Synergy effect between quaternary phosphonium ionic liquid and ammonium polyphosphate toward flame retardant PLA with improved toughness, Coompos. Part, B-Eng. 197 (2020) 108192, https://doi.org/10.1016/j.compositesb.2020.108192.
[56] Z. Jiang, M. Ma, X. Wang, S. Chen, Y. Shi, H. He, X. Wang, Toward flame-retardant and toughened poly(lactic acid)/cross-linked polyurethane blends via the interfacial reaction with the modified bio-based flame retardants, Int. J. Biol. Macromol. 251 (2023) 126206, https://doi.org/10.1016/j.ijbiomac.2023.126206.
[57] R. Mincheva, H. Guemiza, C. Hidan, S. Moins, O. Coulembier, P. Dubois, F. Laoutid, Development of inherently flame-retardant phosphorylated PLA by combination of ring-opening polymerization and reactive extrusion, Materials 13 (1) (2019) 13, https://doi.org/10.3390/ma13010013.